VIRUS: comparison of lab characterization with on-sky performance for multiple spectrograph units

Indahl, Briana, Hill, Gary, Zeimann, Greg, Froning, Cynthia, Gebhardt, Karl, et al.

Briana L. Indahl, Gary J. Hill, Greg Zeimann, Cynthia Froning, Karl Gebhardt, Andreas Kelz, Thomas Jahn, Francesco Montesano, Jan Snigula, Phillip MacQueen, Trent Peterson, Niv Drory, Taylor Chonis, Hanshin Lee, Brian L. Vattiat, Jason Ramsey, Andrew Peterson, "VIRUS: comparison of lab characterization with on-sky performance for multiple spectrograph units," Proc. SPIE 10702, Ground-based and Airborne Instrumentation for Astronomy VII, 1070281 (10 July 2018); doi: 10.1117/12.2313051

SPIE.

Event: SPIE Astronomical Telescopes + Instrumentation, 2018, Austin, Texas, United States

VIRUS: comparison of lab characterization with on-sky performance for multiple spectrograph units

Briana L. Indahl[a], Gary J. Hill[a,b], Greg Ziemann[b], Cynthia Froning[a], Karl Gebhart[a], Andreas Kelz[c], Thomas Jahn[c], Francesco Montesano[d], Jan Snigula[d], Phillip MacQueen[a], Trent Peterson[b], Niv Drory[b], Taylor Chonis[e,a], Hanshin Lee[b], Brian L. Vattiat[b], Jason Ramsey[b], Andrew Peterson[b]

[a]Department of Astronomy, University of Texas at Austin,2515 Speedway Drive, Austin, TX, USA;
[b]McDonald Observatory, University of Texas at Austin, 2515 Speedway Drive, Austin, TX, USA;
[c]Leibniz-Institut Fur Astrophysik, Postdam, Germany;
[d]Max-Planck-Institut fr Extraterrestriche-Physik, Giessenbachstrasse, Germany;
[e]Ball Aerospace, Boulder, CO, USA

ABSTRACT

The Visible Integral Field Replicable Unit Spectrograph (VIRUS), the instrument for the Hobby Eberly Telescope Dark Energy Experiment (HETDEX), consists of 78 replicable units, each with two integral field spectrographs. The VIRUS design takes advantage of large-scale replication of simple units to significantly reduce engineering and production costs of building a facility instrument of this scale. With VIRUS being 156 realizations of the same spectrograph, this paper uncovers the statistical variations in production of these units. Lab relative throughput measures are compared with independently measured grating and optical element performance allowing for potential diagnosis for the cause of variation due to spectrograph elements. Based on variations in performance of individual optical components, throughput curves are simulated for 156 VIRUS spectrograph channels. Once delivered, each unit is paired with a fiber bundle and throughput measurements are made on sky using twilight flats. We compare throughput variance from on-sky measurements to the simulated throughputs. We find that the variation in throughput matches that predicted by modeling of the individual optics performance. This paper presents the results for the 40 VIRUS units now deployed.

Keywords: Hobby-Eberly Telescope, HETDEX, VIRUS, characterization, high-mulitplex,spectrograph, integral field, optical, instrument performance

1. INTRODUCTION

The Hobby Eberly Telescope Dark Energy Experiment (HETDEX) aims to survey nearly 0.8 million Lyman-emitting galaxies from $2.9 < z < 3.5$ to be used as tracers of large scale structure in the universe. In order to survey emission-line objects in the targeted 450 square degree patch of the sky, wide-field integral field spectroscopy is required. To conduct this massive survey, a revolutionary multiplexed instrument, Visible Integral-Field Replicable Unit Spectrograph (VIRUS), is currently being constructed for the 9.2 meter Hobby Eberly Telescope (HET) at McDonald Observatory in West Texas. The instrument design takes advantage of large scale replication of simple units to significantly reduce engineering and production costs of building a facility instrument of this scale for a large telescope.

VIRUS consists of 78 replicable units, each with two integral field spectrographs. Each spectrograph consists of just 3 reflective and 2 refractive optics with dielectric reflective coatings to optimize throughput. Every

Further author information: (Send correspondence to B.L.I.)
B.L.I.: E-mail: blindahl@astro.as.utexas.edu, Telephone: 1 414 232 3958
G.J.H.: E-mail: hill@astro.as.utexas.edu, Telephone: 1 414 471 1477

Ground-based and Airborne Instrumentation for Astronomy VII, edited by Christopher J. Evans, Luc Simard, Hideki Takami,
Proc. of SPIE Vol. 10702, 1070281 · © 2018 SPIE · CCC code: 0277-786X/18/$18 · doi: 10.1117/12.2313051

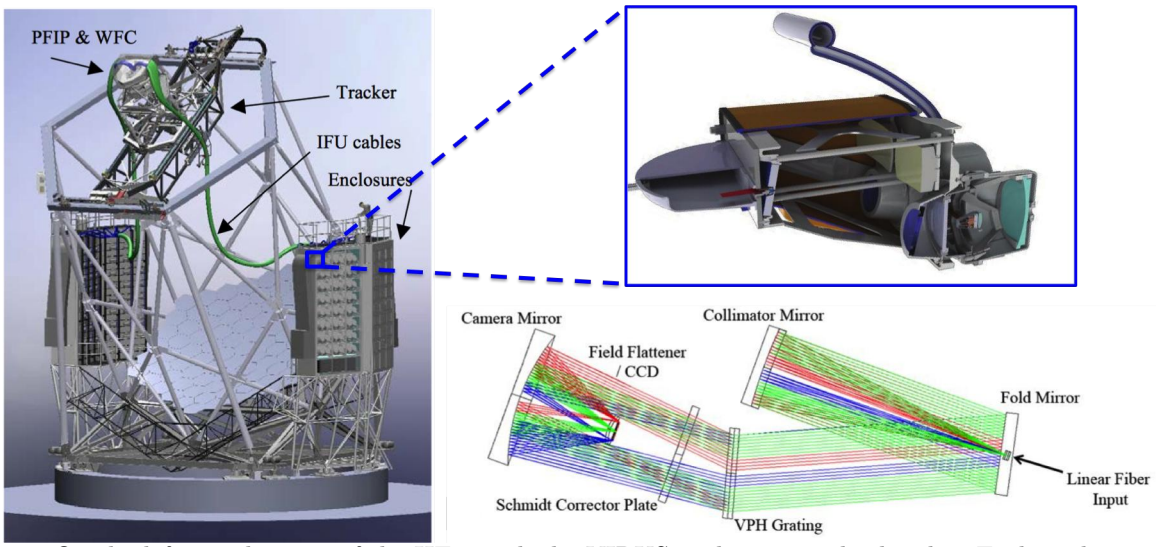

Figure 1: On the left is a drawing of the HET with the VIRUS enclosures on both sides. Each enclosure houses 40 units. A zoom a schematic of a single VIRUS unit is shown on the upper right with its optical layout underneath.[1]

VIRUS unit individually images 448 spectra from its fiber feed covering a spectral range of 350-550nm at $R \sim 750(at 450nm)$.[1–3] In total, the array of 156 VIRUS spectrographs observe the newly upgraded HET's 22 arcmin focal plane[4–6] with a 1/4.5 fill factor. In a single observation with VIRUS, 156 spectrographs image nearly 35,000 spectra.[1–3]

Increasing telescope diameters are demanding larger, more complex spectrographs which require faster cameras and/or larger format CCDs which are expensive and difficult to engineer. This type of massive replication will become a cost effective way to built monolithic instruments for the upcoming class of extremely large telescopes but at the cost of variation of performance between units.[7] With VIRUS being the first largely replicable instrument we have the chance to uncover the statistical variations in production of these units. This paper analyzes performance of the large sets of individual optical components compared to throughput variation measured on sky for the first 40 VIRUS units deployed.

Section 2 briefly describes the optomechanical design of a VIRUS unit. Modeling of VIRUS throughput curves are based on the 6 main optical components of a VIRUS spectrograph. Section 3 provides an overview of those components and a discussion of their performance data. VIRUS performance data taken in lab prior to deployment is discussed in section 4. Section 5 discusses how we predicted VIRUS performance from simulating throughput curves based on optics performance variability. These models are compared to measured on-sky throughputs in section 6. The final section 7 summarizes the results for the first 40 units deployed and the future for VIRUS.

2. VIRUS UNIT DESCRIPTION

Each VIRUS unit is comprised of three main components: the IFU assembly, the collimator (with its environmental housing), and the camera cryostat with its paired controller. An expanded view of the VIRUS components is illustrated in Fig. 2. Each subsystem is discussed in the following subsections:

2.1 IFU assembly

A single VIRUS unit is fed a dense pack fiber bundle containing 448, 266μm (1.5 arcseconds on sky) fibers. Each fiber bundle is arrayed on a 50x50 $arcsec^2$ sky area with a 1/3 fill factor. The 78 VIRUS fiber bundles are about 20 meters long. Each fiber bundle input head is plugged into an input head mount plate above the wide field correcting optics housed on the telescope tracker. The output end of the fiber bundle plugs into the back of the

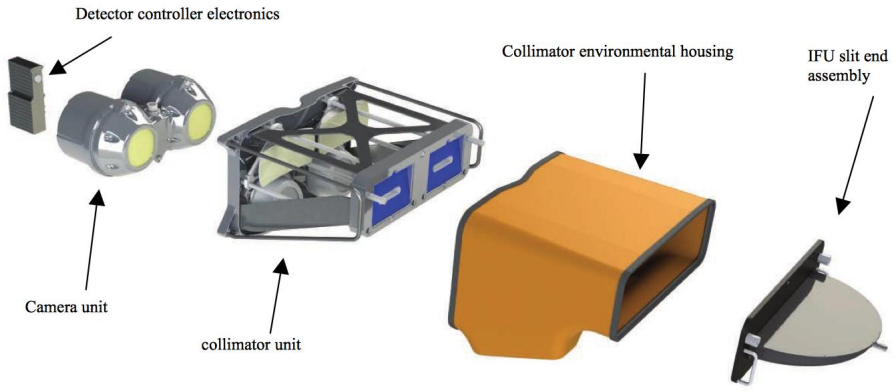

Figure 2: This image is an exploded view of a VIRUS unit highlighting its main components. Starting from the right is the IFU slit assembly which fans out the 448 fibers in the bundle along 2 slits. This feeds light to the back of the collimator covered in a housing to shroud it from stray light. The collimator attaches to the cryostat camera with its paired detector controller shown on the far left.[1]

IFU assembly mounted to the back of a unit. Each spectrograph channel is fed 224 of the 448 fibers fanned along a collimator slit. Refer to Ref. 2, 8 for a more detailed description of the fiber bundles.

2.2 collimator assembly

The collimator housing is shared between the two spectrographs with a baffle separating the channels. Light from the fibers enters through the collimator slit in the back fold mirrors. The pupil is then collimated by the collimator mirror and then reflected off of the fold mirror on the back of the entrance slit. Light is then dispersed through the volume phase holographic (VPH) grating before entering the camera cryostat. Refer to Ref. 9, 10 for a more detailed description of collimator design and build.

2.3 camera cryostat

The two Schmidt design cameras for a VIRUS unit are housed in an aluminum cast vacuum cryostat. The cryostat vacuum is shared between two spectrograph channels significantly reducing the number of vacuum components and seal surfaces, increasing the vacuum lifetime and reducing cost.[1] Refer to Ref. 11 for details of the cryogenic system.

After light is dispersed by the VPH grating it enters the croystat via a window housing a spherical corrector plate. Light is reflected off of a spherical camera mirror, passed through a field flattener and then imaged on the CCD. Four Invar clips mount the fused silica field flattener (FF) lens on top of the CCD. The CCD attaches to an arm protruding into the center of the spider mount. The spider design, is optimized to minimize obstruction of light to the primary spherical mirror. CCD controllers connect through the bulkhead connector controlling the two detectors inside the unit. Refer to Ref. 12, 13 for a more detailed description of the camera cryostat design and build.

3. VIRUS OPTICS DESCRIPTION AND PERFORMANCE

We will discuss the main optical components that will contribute most of the light losses and structure in the resulting throughput curves. Throughout the paper when we model throughput curves we are using the following 6 main optical components:

- **Fiber Bundles (IFUs):** The fibers were assembled and tested at Leibniz Institute for Astrophysics (AIP). Each fiber bundle was delivered with a report assessing its performance overall and on a fiber to fiber basis.[8] These reports present measurements of the relative throughput of each fiber bundle at two wavelengths. Instead of fitting a line through these points we parameterized them based on the typical shape of an IFUs response. This data is presented in Fig. 3 in the panel labeled IFU.

- **Gratings:** Grating were manufactured by Syzygy Optics, LLC. SyZyGy also measured grating efficiencies using a test apparatus that was supplied by UT-Austin. The test setup and results were presented in Ref. 14. Measurements of the grating efficiencies were made at 3 wavelengths and cubic splines were fit to the points for each grating. Cubic splines were chosen as Chonis et. al. 2014 determined this fit was most reflective of the the typical grating efficiency. This data is presented in Fig. 3 in the panel labeled Grating.

- **CCDs:** Each CCDs has a 2064x2064 format with 15μm pixels and 100% fill factor. The University of Arizona Imaging Technology Laboratory is providing backside illuminated CCDs from wafers manufactured by Semiconductor Technology Associates, Inc. The CCDs have AR coatings to optimize the CCDs for the VIRUS bandpass.[15] Each CCD is delivered with a report containing measurements of its quantum efficiency (QE) at 5 wavelength values. A cubic spline was fit to the points as we found this best matched the typical QE curve for our CCDs. This data is presented in Fig. 3 in the panel labeled CCD.

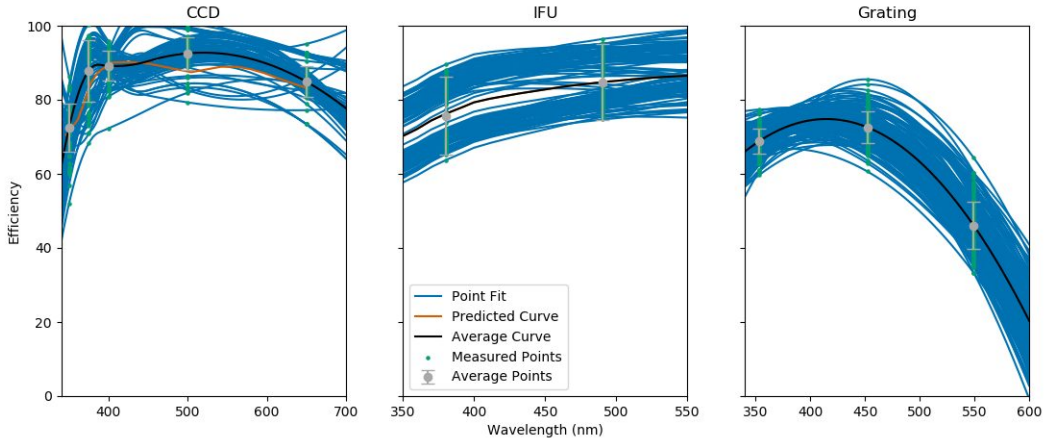

Figure 3: The three panels show the fits to the data (blue curves) for the CCDs, fiber bundles (IFU) and Gratings. The black overplotted curve in each panel represents the average curve with the average (and standard deviation) of the actual measured data points in gray. The CCD and IFU have predicted/typical curves plotted in orange.

- **Fold Mirrors:** The fold mirror has a multi-layer dielectric reflective coating. All of the fold mirrors were coated at PGO. We produced Cary spectrophotometer scans of PGO provided witness samples. These scans are presented in Fig. 4.

- **Collimator and Camera Mirrors:** Both mirrors have a multi-layer dielectric reflective coating like the fold mirror. However, the collimator and camera mirrors were coated at Cascade. We also produced Cary scans of witness samples provided by Cascade (witness). For some of the mirrors that were missing witness samples we instead used reflectance scans provided by Cascade. These scans are presented in Fig. 4. The curves that came from Cary scans of witness samples are referred to in the legend as 'witness'. The curves that came from reflectance scans are referred to in the legend as 'scan'.

For the most part all of the delivered optics discussed above meet or exceed the specifications.

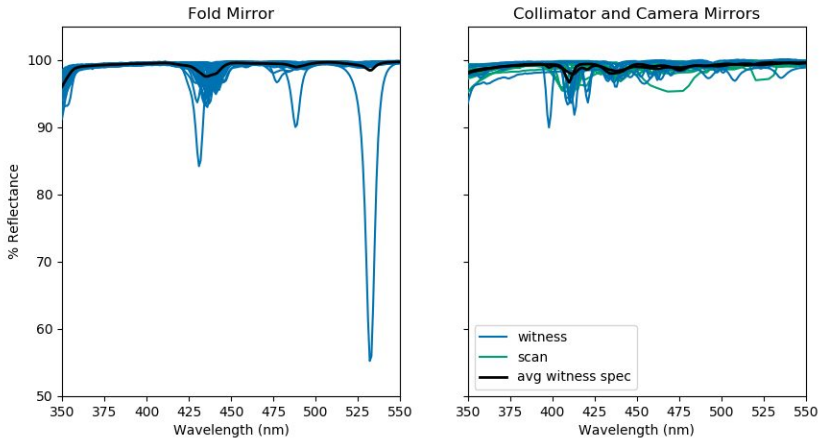

Figure 4: The two panels show the reflectance curves for 3 mirrors in a VIRUS spectrograph. Curves plotted in blue come from Cary scans of witness samples. Curves plotted in green are from scans provided by the manufacturer. The black curves are the average curves for the mirrors.

4. LAB CHARACTERIZATION

As part of the replication process each VIRUS unit progresses through an assembly line of stages before deployment. The first stage is the build of the optical and detector systems which are then mounted into the cryostat. Each one of these camera units is paired with a collimator and moves on to alignment where both a camera an collimator mirror are adjusted for focus and image quality.[13] The final stage before deployment is characterization in lab. Lab characterization consists of many tests discussed in detail in Ref. 16. Here we discuss only the data taken to characterize the units relative system performance.

4.1 lab setup

A separate lab at UT Austin is dedicated to characterization. A light tight room inside this lab houses a cryogenic system for cooling a single unit before and during characterization. The units cryostat is cooled and kept at their on-sky operating temperature of -110 Celsius during data taking. The hardware computer for data taking and the mux sit outside this room to shield the unit from the mux LEDs or screen light. As a final precaution the unit is also covered in a thick black shroud to further guard against any stray light.

VIRUS units are not paired with their respective fiber bundles until deployment to the HET. Each unit in the lab is characterized with the same fiber bundle to properly characterize the detector system without including variance of fiber bundle throughput. Both emission and continuum sources are fed to the fiber bundle end via the Lab Calibration Unit (LCU).

The LCU continuum source is provided by the Laser Driven Light Source (LDLS) (Energetiq EQ-99XFC). The LDLS provides a very uniform and stable source of light across the spectral range of VIRUS and beyond. The continuum source is first fed to a reflective aluminum box essentially acting as a integrating sphere through a 230 micron fiber optic cable. The light exits this cable and enters the compound parabolic concentrator collimated along its axis. The light is output from the LCU through a liquid light guide optimized for the VIRUS spectral range. The unit fibers are coupled to the output liquid light guide through an IFU illuminator assembly.

4.2 relative performance analysis

We ideally wanted to characterize the relative throughput of each of the VIRUS unit using the fiber flats taken in lab. We wanted to measure relative throughputs by summing the counts from the fiber flats. This method assumes that each unit is seeing the same amount of photons for a given exposure time. However, this requires that we trust our set up is extremely stable over long periods of time (several years if want to compare in lab characterization data taken for all VIRUS units) and our set up is repeatable for each unit.

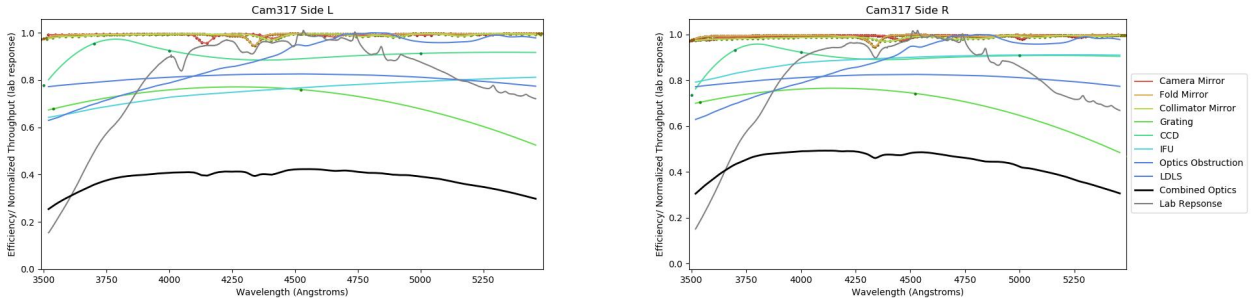

Figure 5: This figure is a breakdown of the efficiency curves for the individual optical components for VIRUS unit 317's left and right spectrograph channel. The combined efficiency based on the optical components is plotted in black. This curve was corrected for the optics obstruction model caused by the CCD being mounted in front of the camera mirror. The gray curves represent the lab measured relative throughputs of that channel normalized to the maximum value in the response curve. This curve contains features of the LDLS lamp used to take the fiber flats these curves were made from. These features could not be taken out since the manufacturer provide LDLS curve (plotted in blue) is much lower resolution than the VIRUS spectrographs. The lab response also contains a significant drop in the UV, compared to the optics combined curve, due to optics in the feed assembly that could not be modeled.

Time series tests of the LDLS show it is stable for over month long periods, however, it is known to degrade over time depending on the number of times it is turned on. It is hard to know how much it has degraded since the first unit characterized. We have also proved that even with careful design our feed setup is somewhat variable for each unit taken in and out of the lab. Full characterization of each unit requires swapping of the fiber feed for a pixel flat head. This means that the LCU liquid light guide output gets unplugged and re-plugged back in to the fiber bundle for each unit. We have proven the way the liquid light guide is plugged into the fiber feed is not as repeatable as we thought. As a result we are not able to make relative throughput measurements from the lab characterization data.

4.3 breakdown of optical components

Since we could not compare relative throughputs between units we analyzed the shape of the measured throughput curve for a given unit. A throughput curve was measured from the fiber flats taken during lab characterization. The flats underwent basic reductions and the fiber spectra were extracted. The counts from each spectra in a given spectrograph channel were summed and and resulting summed spectra were normalized by the maximum value. The normalized lab spectra for the two spectrograph channels in unit 317 are shown in figure 5 as the curve labeled Lab Response.

During the VIRUS builds the serial numbers for each optical component are recorded. For a given built spectrograph we plotted the efficiencies measured for its optical components. Figure 5 shows the efficiency curves for its six major optical components (discussed on Sec. 3) in unit 317's left and right spectrograph channels. We combined these curves to create a predicted efficiency curve for that spectrograph channel (labeled as Combined Optics). The combined curve was corrected for the optics obstruction (model also plotted) due to the CCD mount obstructing light before the camera mirror. This obstruction has a wavelength dependent nature since the light is dispersed by the grating prior to entering the cryostat. Note that the lab response curve is a relative measure normalized to one and combined optics curve is an absolute efficiency measure, so when comparing them we reference their shape since the lab response is not scaled to match the combined optics curve.

It is apparent from comparing the combined curve to the individual optics that the most of the loss in the blue can be attributed to the CCD where the loss on the red end to the grating. The broad dips are due to known absorptions in the mirror coatings. In comparing the combined optics curve to the measured lab response there is a noticeable loss in the UV in the lab response that is not due to the spectrograph optics. We traced this back to optics in the IFU illuminator assembly. These optics are not optimized for the bluer parts of our

spectral range and we do not have manufacturer models of these to remove this feature. Also many of the higher resolution features in the lab measured response are from the LDLS. We tried to remove this spectrum from the lab response with a curve from the manufacturer (plotted as LDLS), however, this curve has a much lower resolution than VIRUS so we could remove the shape of the LDLS but not the higher order features.

Despite efforts for a repeatable and stable setup we decided the best measure for relative performance of the units would be measured on sky where all units observe simultaneously. Since throughput can be analyzed in a relative sense there is no need to build complex models of the light feed (HET) to the spectrographs since it is constant across all units and can be normalized out.

5. PREDICTING VIRUS PERFORMANCE

Before a single VIRUS unit was built and deployed, predictions of throughput were made based purely on the specifications set for the manufacturer of the optics. Now that all of the mirrors, IFUs, gratings, and most of the CCDs have been delivered we measured a typical efficiency curve for each component based on the average of the measurements. We combined the average efficiencies of all the components to create a typical VIRUS throughput curve to compare to the original model based on specifications. This is plotted in figure 6. The throughput curve based on the measured average optics slightly outperforms since the components for the most part met or exceeded specifications.

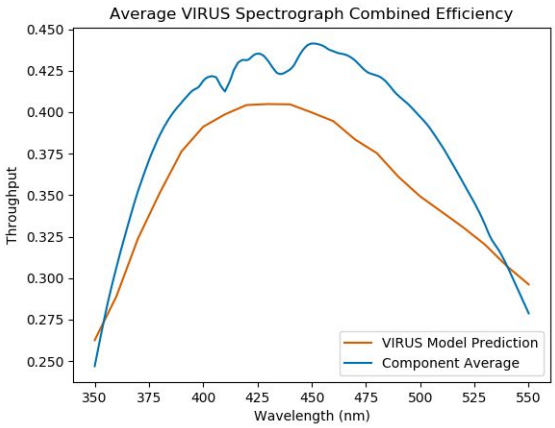

Figure 6: Plotted in blue is the predicted throughput of a VIRUS spectrograph based on the average efficiency of the optical components. This model is compared to the VIRUS predicted throughput based on the specifications for the optics (orange).

Using the data we have on all of the major optical components, we also wanted to model the expected variation in throughput for VIRUS from just the variation in the optical components. We simulated a VIRUS throughput curve by randomly drawing from the component data. For the IFU, CCD, and gratings we built efficiency curves for each component by randomly drawing from the pool of data points. For the CCD and grating, cubic splines were fit to the points since this most closely replicated the typical shape of those component's efficiencies. The IFU curve was parameterized in the same way as described in Sec. 3 based on the two measured points. The statistics available for the mirrors are much smaller due to the measurements being from witness samples of a batch of mirrors and not the individual mirrors. The mirror curves are also much higher resolution than the other components so to preserve the absorption features we just choose randomly from the sample of curves for each mirror. The randomly sampled curves for the individual components were then combined to create the simulated throughput curve.

We randomly generated 156 throughput curves to simulate the entire VIRUS array. This is shown in left plot in figure 7. The average throughput of the 156 curves is plottd in black. We then ran this experiement 500 times and plotted the average curve from each in figure 7's right plot. There is some spread in that average over

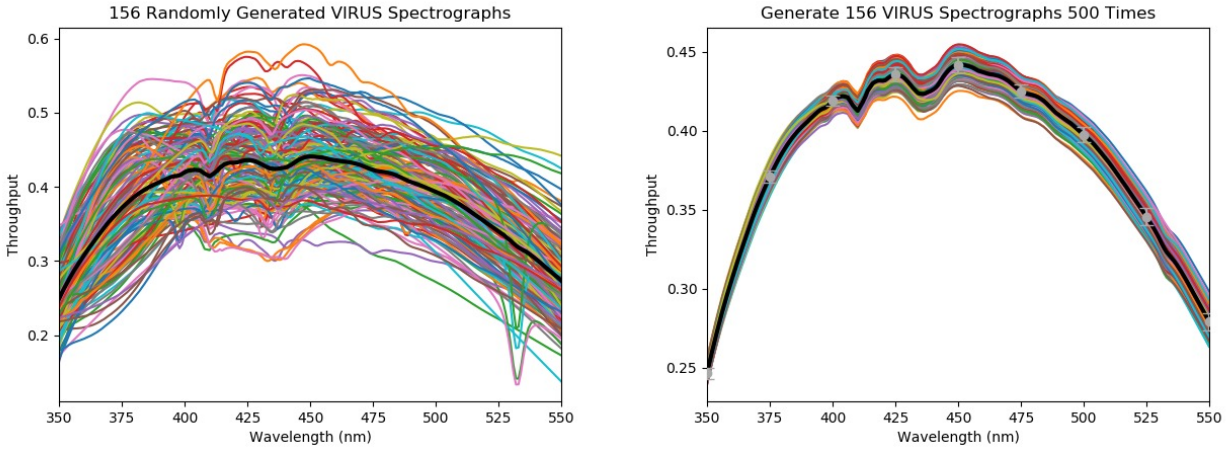

Figure 7: (left) This shows 156 simulated throughput curves for VIRUS spectrographs based on the variation in the measured optics performance. The black curve is the average. (right) This figure shows the spread in the average curve if you run this experiment 500 times. The spread is on the order of a few percent

500 runs but it is only on the order of a few percent. A discussion of the variance in the simulated throughput curves and comparison to on-sky measurements can be found the the following section.

6. ON-SKY PERFORMANCE

Currently 40 units (80 spectrograph channels) are deployed and on-sky at the HET. With a little over half of the array on-sky we proceeded to make relative throughput measures to compare with the simulated curves of the optics.

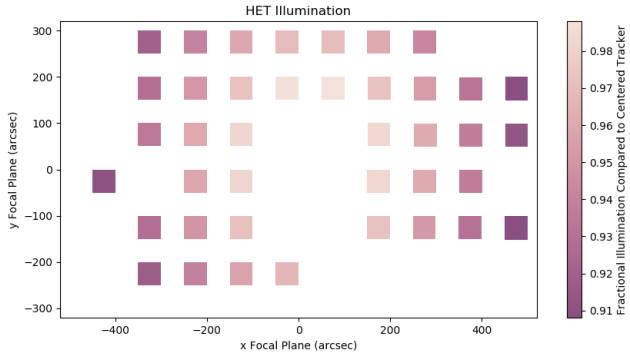

Figure 8: This figure shows a model of the HET field illumination. The image represents a portion of the focal plane of the HET. Each colored box is an IFU that is feeding one of the 40 deployed VIRUS units. The color scale represents the fraction of the HET pupil that IFU sees compared to the fraction of the HET pupil seen at the center of the focal plane. The spread is about 10 percent difference from the more central IFUs to the ones on the edges.

On-sky relative throughput measurements were made from twilight flats taken at the start of the night. It is assumed the twilight sky is flat over the 17 arcminutes of the IFU pattern. The twilight flats were run through basic reduction. Fiber variation was corrected for and all fibers within a channel summed. In order to compare these measures with the simulated spectra, the HET response needed to be taken out. This is for the most part removed during normalization of all of the channels since the twilight data is taken with all channels

simultaneously. However, not every fiber bundle sees the same HET pupil. Fiber bundles near the center of the input head mount plate will see a slightly larger fraction of the HET mirror than fiber bundles near the edge. We applied a correction for the HET field illumination to each channel. The output of the model of the field illumination can be seen in figure 8. Each channels response was then normalized by the average channel. This normalization removes the HET response common to all channels leaving behind the relative responses of the 80 VIRUS channels. We normalize the simulated VIRUS throughputs by the their average to compare to the normalized throughputs from on-sky measurements. Both results are shown in figure 9. These plots essentially show the spread in throughput as a function a wavelength. The variation in throughput matches that predicted by modeling of the individual optics performance.

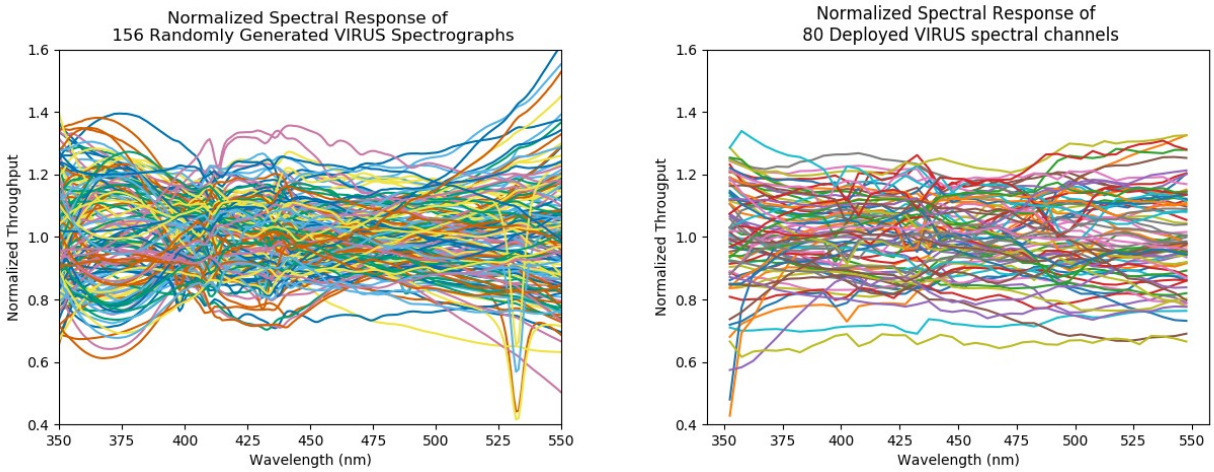

Figure 9: (left) This plot shows the spectral response of the 156 simulated throughput curves shown in Fig. 7 normalized by the average curve. (right) This shows the normalized response of the 80 deployed VIRUS spectrograph channels measured on sky. These curves are corrected for the HET illumination so they can be directly compared to the simulated curves.

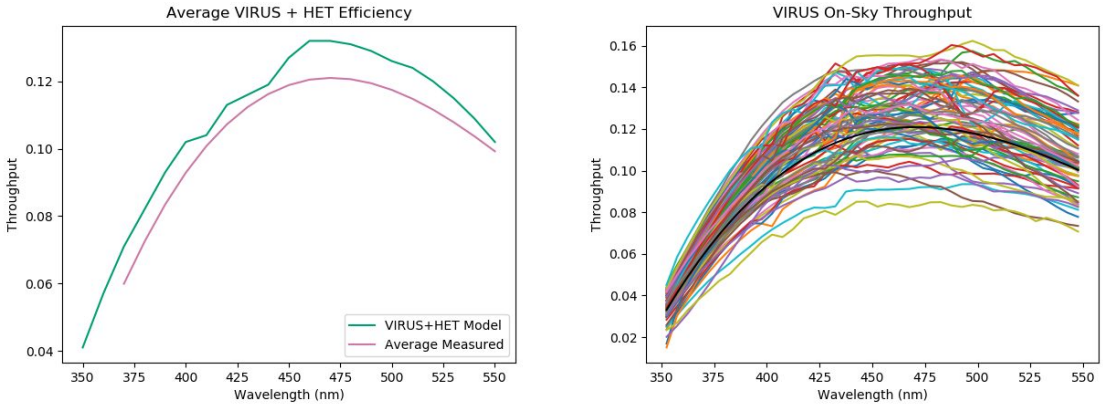

Figure 10: (left) Plotted in green is the same model of the VIRUS throughput based on optics specifications in Fig. 6 but including a model of the HET assuming a degradation in the HET mirror segments. This model is compared to a measure of the average absolute throughput of VIRUS calibrated from LRS2 plotted in pink. (right) This plot shows the approximate absolute throughput measures of the 80 VIRUS spectrographs deployed. These curves were made from the on-sky measured normalized throughput curves in Fig. 9 multiplied by the average absolute throughput of VIRUS

The average on-sky throughput of the deployed VIRUS units is derived in comparison with the LRS2 integral field spectrograph correcting for the field illumination of the HET. LRS2 has completed commissioning and its throughput has been very well calibrated. The left plot in figure 10 compares the average VIRUS absolute throughput on the HET (labeled Average Measured) with the VIRUS model based on the optics specifications plus a model of the HET. The HET model assumes some fraction of HET mirror degradation. It is possible that the small offset between the model and the measurements are due to the HET mirrors being more degraded than the model assumption, however, it is hard to be certain. The right plot in figure 10 shows the approximate absolute throughput of the 80 VIRUS spectrograph channels. This was generated by multiplying the normalized responses by the average absolute throughput measure.

7. SUMMARY

After assessment of each set of optical components including the fiber bundles, gratings, CCDs, and 3 multi-layer dielectric reflective coated mirrors we find that for the most part the batches of components meet or exceed expectations. As a result, a typical throughput curve built from the average efficiencies of the individual optics outperforms the predicted VIRUS throughput based on the specifications.

In an effort to assess the performance of the built VIRUS spectrographs we attempted to measure throughput curves from lab characterization data. Due to not having a reliably stable and repeatable lab setup we found it best to use on-sky data to compare performance between multiple units.

Based on just the variability in the optics performance we simulated throughput curves for 156 VIRUS spectrographs. By normalizing these values by their average curve we were able to compare the spread in the simulated throughput with the spread in throughput measured on sky for the 80 spectrograph channels deployed. We found that the spread in throughput from just the variation in the optics matches that measured on sky.

VIRUS provides a first and currently unique opportunity to understand the performance of spectrographs replicated on a 100-fold scale. Such instruments have applications on future extremely large telescopes. The experience with VIRUS is that it is possible to predict the performance and, with care in specifying component requirements, achieve the expectations on-sky.

ACKNOWLEDGMENTS

HETDEX is run by the University of Texas at Austin McDonald Observatory and Department of Astronomy with participation from the Ludwig-Maximilians-Universitt Mnchen, Max-Planck-Institut fr Extraterrestriche-Physik (MPE), Leibniz-Institut fr Astrophysik Potsdam (AIP), Texas A&M University (TAMU), Pennsylvania State University, Institut fr Astrophysik Gttingen, University of Oxford and Max-Planck-Institut fr Astrophysik (MPA). In addition to Institutional support, HETDEX is funded by the National Science Foundation (grant AST-0926815), the State of Texas, the US Air Force (AFRL FA9451-04-2-0355), by the Texas Norman Hackerman Advanced Research Program under grants 003658-0005-2006 and 003658-0295-2007, and by generous support from private individuals and foundations.

We thank the staffs of McDonald Observatory, HET, AIP, MPE, TAMU, IAG, Oxford University Department of Physics, the University of Texas Center for Electromechanics, and the University of Arizona College of Optical Sciences and Imaging Technology Lab for their contributions to the development of the WFU and VIRUS.

REFERENCES

[1] Hill, G. J., Tuttle, S. E., Drory, N., Lee, H., Vattiat, B. L., DePoy, D. L., Marshall, J. L., Kelz, A., Haynes, D., Fabricius, M. H., Gebhardt, K., Allen, R. D., Anwad, H., Bender, R., Blanc, G., Chonis, T., Cornell, M. E., Dalton, G., Good, J., Jahn, T., Kriel, H., Landriau, M., MacQueen, P. J., Murphy, J. D., Peterson, T. W., Prochaska, T., Nicklas, H., Ramsey, J., Roth, M. M., Savage, R. D., and Snigula, J., "VIRUS: production and deployment of a massively replicated fiber integral field spectrograph for the upgraded Hobby-Eberly Telescope," *Proc. SPIE* **9147**, 27 (2014).

[2] Hill, G. J., Tuttle, S. E., Vattiat, B. L., Drory, N., Kelz, A., Ramsey, J., DePoy, D. L., Marshall, J. L., Gebhardt, K., Chonis, T., Dalton, G., Farrow, D., Good, J., Haynes, D., Indahl, B., Jahn, T., Kriel, H., Montesano, F., Nicklas, H., Noyola, E., Prochaska, T., Allen, R. D., Blanc, G., Fabricius, M. H., Landriau, M., MacQueen, P. J., Roth, M. M., Savage, R. D., and Snigula, J., "VIRUS: first deployment of the massively replicated fiber integral field spectrograph for the upgraded Hobby-Eberly Telescope," *Proc. SPIE* **9908**(54) (2016).

[3] Hill, G. J., Kelz, A., Lee, H., MacQueen, P. J., Peterson, T., Ramsey, J., Vattiat, B. L., DePoy, D. L., Drory, N., Gebhardt, K., Good, J. M., Jahn, T., Kriel, H., Marshall, J. L., Montesano, F., Tuttle, S. E., Balderrama, E., Chonis, T. S., Dalton, G. B., Fabricius, M. H., Farrow, D., Fowler, J. R., Froning, C., Haynes, D. M., Indahl, B. L., Martin, J., Montesano, F., Mrozinski, E., Nicklas, H., Noyola, E., Odewahn, S., Peterson, A., Prochaska, T., Shetrone, M., Smith, G., Snigula, J. M., Spencer, R., and Zeimann, G., "VIRUS: status and performance of the massively replicated fiber integral field spectrograph for the upgraded Hobby-Eberly telescope," **10702**(56) (2018).

[4] Hill, G. J., Drory, N., Good, J., Lee, H., Vattiat, B. L., Kriel, H., Ramsey, J., Randy Bryant, R., Elliott, L., Fowler, J., Landriau, M., Leck, R., Odewahn, S., Perry, D., Savage, R., Schroeder Mrozinski, E., Shetrone, M., Damm, G., Gebhardt, K., MacQueen, P., Martin, J., Armandroff, T., and Ramsey, L., "The Hobby-Eberly Telescope wide-field upgrade," *Proc. SPIE* **9906**(5) (2016).

[5] Lee, H., Hill, G. J., Good, J., Vattiat, B., Shetrone, M., Martin, J., Schroeder Mrozinski, E., Kriel, H., Oh, C.-J., Frater, E., Smith, B., and Burge, J., "Delivery, installation, on-sky verification of Hobby Eberly Telescope wide-field corrector," *Proc. SPIE* **9906**(156) (2016).

[6] Hill, G. J., Drory, N., Good, J. M., Lee, H., Vattiat, B. L., Kriel, H., Ramsey, J., Bryant, R., Fowler, J. R., Landriau, M., Leck, R., Mrozinski, E., Odewahn, S., Shetrone, M., Westfall, A., Terrazas, E., Balderrama, E., Buetow, B., Damm, G., MacQueen, P. J., Martin, J., Martin, A., Smither, K., Rostopchin, S., Smith, G., Spencer, R., Armandroff, T., Gebhardt, K., and Ramsey, L. W., "Completion and performance of the Hobby-Eberly telescope wide field upgrade," **10700**(20) (2018).

[7] Hill, G. J., "Replicated spectrographs in astronomy," *Advanced Optical Technologies* **3**, 265–278 (June 2014).

[8] Kelz, A., Jahn, T., Haynes, D., Hill, G. J., Lee, H., Murphy, J. D., Neumann, J., Nicklas, H., Rutowskaa, M., Sandin, C., Streicher, O., Tuttle, S. E., Fabricius, M., Bauer, S. M., Vattiat, B. L., Anwand, H., and Savage, R., "HETDEX / VIRUS: testing and performance of 33,000 optical fibres," *Proc. SPIE* **9147**(75) (2014).

[9] Lee, H., Hill, G. J., Marshall, J. L., Vattiat, B. L., and DePoy, D. L., "Visible Integral-field Replicable Unit Spectrograph (VIRUS) optical tolerance," in [*Ground-based and Airborne Instrumentation for Astronomy III*], **7735**, 77353X (July 2010).

[10] Marshall, J. L., DePoy, D. L., Prochaska, T., Allen, R. D., Williams, P., Rheault, J.-P., Li, T., Nagasawa, D. Q., Akers, C., Baker, D., Boster, E., Campbell, C., Cook, E., Elder, A., Gary, A., Glover, J., James, M., Martin, E., Meador, W., Mondrik, N., Rodriguez-Patino, M., Villanueva, S., Hill, G. J., Tuttle, S., Vattiat, B., Lee, H., Chonis, T. S., Dalton, G. B., and Tacon, M., "VIRUS instrument collimator assembly," in [*Ground-based and Airborne Instrumentation for Astronomy V*], **9147**, 91473S (July 2014).

[11] Smith, M. P., Mulholland, G. T., Booth, J. A., Good, J. M., Hill, G. J., MacQueen, P. J., Rafal, M. D., Savage, R. D., and Vattiat, B. L., "The cryogenic system for the virus array of spectrographs on the hobby-eberly telescope," *Proc. SPIE* **7018**, 9 (2008).

[12] Tuttle, S. E., Allen, R. D., Chonis, T. S., Cornell, M. E., DePoy, D. L., Hill, G. J., Lee, H., Marshall, J. L., Prochaska, T., Rafal, M. D., Savage, R. D., and Vattiat, B. L., "Initial results from VIRUS production spectrographs," in [*Ground-based and Airborne Instrumentation for Astronomy IV*], **8446**, 84465S (Sept. 2012).

[13] Tuttle, S. E., Hill, G. J., Lee, H., Vattiat, B., Noyola, E., Drory, N., Cornell, M., Peterson, T., Chonis, T., Allen, R., Dalton, G., DePoy, D., Edmonston, D., Fabricius, M., Haynes, D., Kelz, A., Landriau, M., Lesser, M., Leach, B., Marshall, J., Murphy, J., Perry, D., Prochaska, T., Ramsey, J., and Savage, R., "The construction, alignment, and installation of the virus spectrograph," *Proc. SPIE* **9147**, 13 (2014).

[14] Chonis, T. S., Frantz, A., Hill, G. J., Clemens, J. C., Lee, H., Tuttle, S. E., Adams, J. J., Marshall, J. L., DePoy, D. L., and Prochaska, T., "Mass production of volume phase holographic gratings for the VIRUS spectrograph array," *Proc. SPIE* **9151**, 91511J (July 2014).

[15] Lesser, M., "Recent astronomical detector development at the university of arizona," *Proc. SPIE* **8453**, 14 (2012).

[16] Indahl, B. L., Hill, G. J., Drory, N., Gebhardt, K., Tuttle, S., Ramsey, J., Ziemann, G., Chonis, T., Peterson, T., Peterson, A., Vattiat, B. L., Li, H., and Hao, L., "VIRUS characterization development and results from first batches of delivered units," in [*Ground-based and Airborne Instrumentation for Astronomy VI*], **9908**, 990880 (Aug. 2016).